

This article was downloaded by:

On: 25 January 2011

Access details: Access Details: Free Access

Publisher Taylor & Francis

Informa Ltd Registered in England and Wales Registered Number: 1072954 Registered office: Mortimer House, 37-41 Mortimer Street, London W1T 3JH, UK



Separation Science and Technology

Publication details, including instructions for authors and subscription information:

<http://www.informaworld.com/smpp/title~content=t713708471>

Modeling of Supercritical Fluid Extraction from *Hippophae rhamnoides* L. seeds

Jianzhong Yin^a; Xianwen Sun^a; Xinwei Ding^a; Hanhua Liang^b

^a School of Chemical Engineering, Dalian University of Technology, Dalian, P.R. China ^b Department of Applied Biology and Chemical Technology, The Hong Kong Polytechnic University, Kowloon, Hong Kong

Online publication date: 10 September 2003

To cite this Article Yin, Jianzhong , Sun, Xianwen , Ding, Xinwei and Liang, Hanhua(2003) 'Modeling of Supercritical Fluid Extraction from *Hippophae rhamnoides* L. seeds', Separation Science and Technology, 38: 16, 4041 – 4055

To link to this Article: DOI: 10.1081/SS-120024718

URL: <http://dx.doi.org/10.1081/SS-120024718>

PLEASE SCROLL DOWN FOR ARTICLE

Full terms and conditions of use: <http://www.informaworld.com/terms-and-conditions-of-access.pdf>

This article may be used for research, teaching and private study purposes. Any substantial or systematic reproduction, re-distribution, re-selling, loan or sub-licensing, systematic supply or distribution in any form to anyone is expressly forbidden.

The publisher does not give any warranty express or implied or make any representation that the contents will be complete or accurate or up to date. The accuracy of any instructions, formulae and drug doses should be independently verified with primary sources. The publisher shall not be liable for any loss, actions, claims, proceedings, demand or costs or damages whatsoever or howsoever caused arising directly or indirectly in connection with or arising out of the use of this material.

Modeling of Supercritical Fluid Extraction from *Hippophae rhamnoides* L. Seeds

Jianzhong Yin,^{1,*} Xianwen Sun,¹ Xinwei Ding,¹
and Hanhua Liang²

¹School of Chemical Engineering, Dalian University of Technology,
Dalian, Liao Ning, P.R. China

²Department of Applied Biology and Chemical Technology,
The Hong Kong Polytechnic University, Kowloon, Hong Kong

ABSTRACT

Modeling of supercritical CO_2 extraction of *Hippophae rhamnoides* L. seed oil was studied at 15 to 30 MPa and 30 to 45°C. Four mean *Hippophae rhamnoides* L. particle sizes ranging from 0.4 to 1.0 mm were tested. CO_2 flow rate ranged between 0.05 and 0.2 $\text{m}^3 \text{ h}^{-1}$. A new method that can be used for the simulation of SCFE process was presented. The model was based on differential mass balances along the extraction bed. The equilibrium between the solid and the fluid phase

*Correspondence: Jianzhong Yin, School of Chemical Engineering, Dalian University of Technology, Dalian 116012, Liao Ning, P.R. China; E-mail: yinjzhaq@mail.dlptt.ln.cn.

appeared to be the controlling step during the extraction fast period. By a series of transforms and derivatives, the explicit expression of the oil yield, $q(z,t)$, was obtained. It can be used for the SCFE process simulation. In this model, only one adjustable parameter was used: the equilibrium constant between the solvent and the free solute phase, K . A fairly good fitting of the experimental data was obtained by setting $K = 10$. The *Hippophae rhamnoides* L. seed oil extraction process was modeled as a desorption process from the seed matter plus a small mass-transfer resistance.

Key Words: Simulation; Supercritical fluid extraction; *Hippophae rhamnoides* L. seed.

INTRODUCTION

Hippophae rhamnoides L. is largely grown in the northeastern and northwestern parts of China. It not only can be used as shelterbelt, its sarcocarp and seeds also have high medical value. To date, *Hippophae rhamnoides* L. seed oil has found widespread use in anticancer and immunity and there is a great demand for *Hippophae rhamnoides* L. seed oil market. In 1997, *Hippophae rhamnoides* L. was listed in the pharmacopoeia of the People's Republic of China. Since then, the extraction of *Hippophae rhamnoides* L. seed oil has attracted much interest, both in research and in industrial processing.

Supercritical carbon dioxide has been used widely in the extraction of oils from natural plants seeds, due to its high efficiency and environmentally benign nature. In this research field, many experiments have been carried out^[1-9] and various factors, such as temperature, pressure, and others, have been investigated. Based on the experimental data, various mathematical models have been proposed to simulate the extraction process. In these models, the most widely used one is based on the mass balances of differential extraction bed. Bulley^[10] extracted oils from canola with supercritical fluid and presented a model based on mass balances, in which he neglected the influence of axial concentration distribution, and suggested that the control factor was the dissolution rate in fluid phase when the grain was big, and if the grain was small, the overall mass-transfer coefficient could be used to describe the transfer process. Roy^[11] found that the mass-transfer process was different, with the solute concentration changed greatly in the solid phase. In the first period of the extraction, the concentration of the solute in the solid phase is large so the mass transfer is controlled by the dissolution equilibrium in the fluid



phase. Goto^[9] and Sovova^[12] have the same viewpoint, and they thought that the concentration of the solute in the solid matrix and the solubility of solute in the fluid phase were the key factors in the whole extraction process.

The mass balance model can be expressed in a series of differential equations, and its conventional solutions should be obtained by means of numerical analysis. Roy^[11] regarded the difference between the solubility and the concentration in the solid phase as the driving force of the mass transfer and he got a numerical result by way of a dimensionless transform making use of the Crank–Nicholson rule. Perrut et al.^[13] got a relation between the extraction time and the solute concentration in the fluid phase and the solid phase, respectively. In an experiment of essential oil extraction from clove, Reverchon^[14] got an analytical solution using the Laplace transform. Regarding the mass-transfer rate as the function of the fluid phase concentration and its solubility, Sovova^[12] used the dimensionless transform to simplify the mass balances model, and got an exact analytical solution of the concentration in the solid phase. Recently, Reverchon et al.^[15] proposed a method to simulate the SCFE process in which only one adjustable parameter k_i was used and microscopic information of seed structure was considered at the same time. Cocco et al.^[16] used the Laplace transform and finite differences method to obtain the mathematical resolution of the desorption model equations of SCFE.

The aim of this work was to propose a new method to resolve the differential equations of mass balances for SCFE by the use of mathematics directly. For this approach, the extraction process was separated into two parts. In each part, the analytical expression of the concentration in the solid phase was proposed. Finally, the calculation results were tested with the experimental data.

MATHEMATICAL MODELS OF EXTRACTION

Extraction Model

To simplify the model, we make some assumptions. Under the same conditions of the extraction and the desorption, the productions may have similar physical properties, thus, the outputs in one extraction process can be regarded as a single compound. We assume that the fluid flows uniformly through the cross-section of the bed, and neglect the pressure drop and temperature gradient along the bed. To minimize the errors caused by this assumption, some 0.4-mm diameter stainless-steel bead packing was



placed in the entrance of the bed uniformly. Considering that the volume of the material was not changed during the extraction process, the void fraction of the bed was considered as a constant. When the concentration distribution along the bed radial was neglected, the concentration in the fluid phase was just dealt with as a function of the extraction time and the distance from the entrance of the bed.

The velocity of the supercritical fluid in the bed is u (m/s), the cross-section area of the bed is A (m^2), an oil mass balance for the solvent phase over an element δh of extractor height is as follows (Figure 1). Thus, the equation of mass balances in an element of the bed is:

$$\rho_f u \frac{\partial c}{\partial z} - \rho_f D_L \varepsilon \frac{\partial^2 c}{\partial z^2} + \rho_f \varepsilon \frac{\partial c}{\partial t} + \rho_s (1 - \varepsilon) \frac{\partial q}{\partial t} = 0 \quad (1)$$

The mass balance equation in solid phase is:

$$\rho_s (1 - \varepsilon) \frac{\partial q}{\partial t} = -f(c, q) \quad (2)$$

When the extraction process is controlled by the dissolution equilibrium in fluid phase,

$$f(c, q) = A_p k_f \rho_f (c^*(q) - c) \quad (3)$$

In Eq. 3, A_p is the specific interfacial area (m^{-1}). If the grain is spherical, $A_p = 6(1 - \varepsilon)/d_p$, where d_p is the mean diameter of the grain and $c^*(q)$ is the

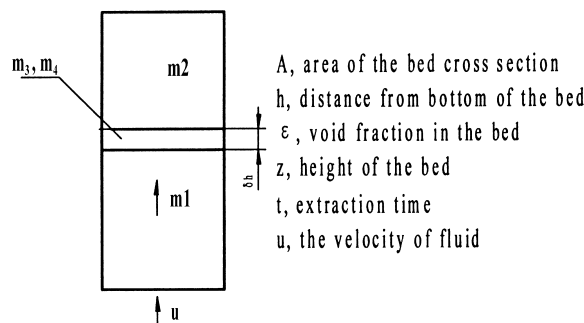


Figure 1. Schematic diagram of the extraction bed.

solute concentration in the fluid phase contributed to the solute, which attached on the solid surface. k_f is the mass-transfer coefficient in the solvent phase and can be calculated with the following formula:

$$k_f \cdot A_p = 2.7 \times 10^{-3}$$

The initial and boundary conditions for the above equations are $t = 0$, $c(0, z) = 0$, $q(0, z) = q_0$, $z = 0$, and $c(t, 0) = 0$.

These conditions mean that at the very beginning of the extraction process, i.e., $t = 0$, the solute concentration in the fluid phase is equal to zero, and in the solid phase, it is equal to q_0 . While at the entrance of the bed, i.e., $z = 0$, the concentration in the fluid phase is equal to zero. It is generally accepted that the solute concentration at the surface of the solid phase is proportional to the solute concentration in the solid phase, $q = K c^*(q)$, where K is the equilibrium constant. For a detailed description of the calculation for K , see a later discussion.

Mathematical Representation

The extraction bed can be looked at as a fixed bed when the fluid velocity in the bed is at about 10^{-4} to 10^{-5} m/s, and the axial dispersion coefficient D_L is at about 10^{-7} to 10^{-9} m/s². To simplify the mathematical solution, we neglect the effect of the axial dispersion. Therefore, we decided to perform modeling without considering the axial dispersion.^[15]

Assume that $A = u\rho_f$, $D = \rho_f \epsilon$, $E = \rho_s(-\epsilon)$, and $F = A_p k_f \rho_f$, then, from Eqs. 2 and 3, we have

$$\begin{aligned} c &= \frac{q}{K} + \frac{E}{F} \frac{\partial q}{\partial t} \\ \frac{\partial c}{\partial t} &= \frac{1}{K} \frac{\partial q}{\partial t} + \frac{E}{F} \frac{\partial^2 q}{\partial t^2} \\ \frac{\partial c}{\partial z} &= \frac{1}{K} \frac{\partial q}{\partial z} + \frac{E}{F} \frac{\partial^2 q}{\partial t \partial z} \end{aligned}$$

When neglecting the effect of axial dispersion, i.e., set $D_L = 0$, Eq. 1 can be transformed to the following type

$$\frac{ED}{F} \frac{\partial^2 q}{\partial t^2} - \frac{EA}{F} \frac{\partial^2 q}{\partial t \partial z} + \left(\frac{D}{K} + E \right) \frac{\partial q}{\partial t} - \frac{A}{K} \frac{\partial q}{\partial z} = 0 \quad (4)$$



Based on the eigenvalue theory, and let $\xi = z$, $\eta = z - (A/D)t$, then the Jacobian equation is:

$$J = \frac{D(\xi, \eta)}{D(z, t)} = \begin{vmatrix} \xi_z, \xi_t \\ \eta_z, \eta_t \end{vmatrix} = -\frac{A}{D} \neq 0$$

Consequently,

$$q(\xi, \eta) = \exp(\alpha\xi + \beta\eta)m(\xi, \eta)$$

and

$$\alpha = \frac{F}{A}, \quad \beta = -\frac{DF}{KEA}$$

Then, we can obtain Eq. 5:

$$\frac{EA}{FD} \frac{\partial^2 m}{\partial \eta \partial \xi} + \frac{F}{KA} m = 0 \quad (5)$$

Eq. 5 is a problem concerned with both an initial and boundary conditions for function $m(\xi, \eta)$, so, Eqs. 1 and 2 can be resolved in this way.

$$\begin{aligned} \frac{\partial^2 m}{\partial \eta \partial \xi} + \frac{DF}{KEA} m &= 0 \\ m(\xi, \eta)|_{\xi=\eta} &= q_0 \exp(-(\alpha + \beta)\xi) \\ \left. \frac{\partial m}{\partial \eta} \right|_{\xi=\eta} &= 0 \\ m(\xi, \eta)|_{\xi=0} &= q_0 \end{aligned} \quad (6)$$

Take into the difference operator:

$$L \equiv \frac{\partial^2}{\partial x \partial y} + a(x, y) \frac{\partial}{\partial x} + b(x, y) \frac{\partial}{\partial y} + c(x, y)$$

In this equation, all of the a, b, and c are functions of x and y, L is the second-order linear operator.

Thus

$$L^* \equiv \frac{\partial}{\partial x \partial y} - a(x, y) \frac{\partial}{\partial x} - b(x, y) \frac{\partial}{\partial y} + c(x, y)$$



and L^* is the conjugate difference operator of L . Furthermore, we can select a function, $v(\xi, \eta, \xi_0, \eta_0)$, that satisfies the following conditions:

$$\begin{aligned} L^*v &= 0 \\ \frac{\partial v}{\partial \xi} |_{\eta} = \eta_0 &= 0 \\ \frac{\partial v}{\partial \eta} |_{\xi} = \xi_0 &= 0 \\ v(\xi, \eta) |_{\xi = \xi_0, \eta = \eta_0} &= 1 \end{aligned} \tag{7}$$

Let $\lambda = DF/KEA$ and assume $v = v(z)$, where $z = z(\xi, \eta) = \sqrt{(\xi - \xi_0)(\eta - \eta_0)}$ and we can get a zero-order Bessel equation:

$$v(\xi, \eta) = J_0(\sqrt{4\lambda Z}) = J_0(\sqrt{4\lambda(\xi - \xi_0)(\eta - \eta_0)}) \tag{8}$$

Assume that $x = \sqrt{4\lambda(\xi - \xi_0)(\eta - \eta_0)}$, then Eq. 8 can be expressed as:

$$J_0(x) = \sum_{k=0}^{\infty} \frac{(-1)^k}{(k!)^2} \left(\frac{x}{2}\right)^2 = 1 - \left(\frac{x}{2}\right)^2 + \frac{1}{(2!)^2} \left(\frac{x}{2}\right)^4 - \frac{1}{(3!)^2} \left(\frac{x}{2}\right)^6 + \dots$$

Solving the derivative of Eq. 6 to ξ along the direction of $\xi = \eta$ (Figure 2) and the integral result along the direction of $\xi = \eta$ from Q to P. Then we have

$$\begin{aligned} m(\xi_0, \eta_0) &= \frac{1}{2} q_0 [\exp(-(\alpha + \beta)\xi_0) + \exp(-(\alpha + \beta)\eta_0)] \\ &\quad - \frac{1}{2} \int_{\eta_0}^{\xi_0} q_0 l^{-(\alpha + \beta)\xi} \frac{\sqrt{\lambda}(\xi_0 - \eta_0)}{\sqrt{(\xi - \xi_0)(\eta - \eta_0)}} \\ &\quad \times J'_0(\sqrt{4\lambda(\xi - \xi_0)(\eta - \eta_0)}) d\xi \\ &\quad + \frac{1}{2} \int_{\eta_0}^{\xi_0} -(\alpha + \beta) q_0 l^{-(\alpha + \beta)\xi} J_0(\sqrt{4\lambda(\xi - \xi_0)(\eta - \eta_0)}) d\xi \end{aligned}$$

where

$$\xi = z, \eta = z - \frac{A}{D}t$$



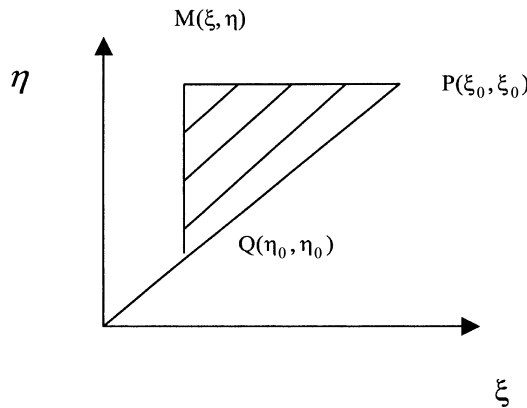


Figure 2. Diagram of the reference coordinate.

Replace point(ξ_0, η_0) with point (ξ, η), then take variables z and t :

$$\begin{aligned}
 m(z, t) = & \frac{1}{2} q_0 [\exp(-(a + \beta)z) + \exp(-(a + \beta)(z - \frac{A}{D}t))] \\
 & - \frac{1}{2} \int_{z - \frac{A}{D}t}^z q_0 l^{-(a + \beta)\tau} \frac{\sqrt{\lambda} \frac{A}{D} t}{\sqrt{(\tau - z)(\tau - z + \frac{A}{D}t)}} \\
 & \times J'_0 \left(\sqrt{4\lambda(\tau - z) \left(\tau - z + \frac{A}{D}t \right)} \right) d\tau \\
 & + \frac{1}{2} \int_{z - \frac{A}{D}t}^z -(\alpha + \beta) q_0 l^{-(\alpha + \beta)\tau} \\
 & \times J_0 \left(\sqrt{4\lambda(\tau - z) \left(\tau - z + \frac{A}{D}t \right)} \right) d\tau
 \end{aligned}$$

and

$$q(z, t) = \exp \left(\alpha z + \beta \left(z - \frac{A}{D}t \right) \right) m(z, t)$$

Assume

$$f(\tau) = \frac{1}{\sqrt{(\tau-z)(\tau-z+\frac{A}{D}t)}} J_0\left(\sqrt{4\lambda(\tau-z)\left(\tau-z+\frac{A}{D}t\right)}\right)$$

So, we can get the analyzed expression of $q(z,t)$

$$\begin{aligned} q(z,t) &= \frac{1}{2} q_0 \exp\left(\alpha z + \beta\left(z - \frac{A}{D}t\right)\right) \\ &\times \left\{ \exp(-(\alpha + \beta)z) + \exp\left(-(\alpha + \beta)\left(z - \frac{A}{D}t\right)\right) \right. \\ &\times \sqrt{\lambda} \frac{A}{D} t \int_{z-\frac{A}{D}t}^z \exp(-(\alpha + \beta)\tau) \times f(\tau) d\tau (\alpha + \beta) \\ &\times \left. \int_{z-\frac{A}{D}t}^z \exp(-(\alpha + \beta)\tau) J_0\left(\sqrt{4\lambda(\tau-z)\left(\tau-z+\frac{A}{D}t\right)}\right) d\tau \right\} \end{aligned} \quad (9)$$

here,

$$x = \sqrt{4\lambda(\tau-z)\left(\tau-z+\frac{A}{D}t\right)} \in (-1, 1)$$

When x lies between -1 and 1 , the function of $q(z,t)$ has a convergent solution.

EXPERIMENTAL

Extraction measurements were carried out in a semi-batch flow extraction apparatus. Supercritical carbon dioxide was used as solvent. Liquid carbon dioxide from the supply cylinder passes through a cold bath (at 263°K), then is pumped with a two-plug pump (Model 2JX-40/8, Hangzhou, P.R. China) and heated by a tubular heat exchanger to the extraction temperatures. The pressure is controlled with a back-pressure regulator (Yancheng, Jiangsu, P.R. China, Model H21X-100P, DW6).



The extractor containing the raw material to be extracted was thermostatically controlled by an electrical heating belt. The temperature inside the extractor was controlled by a digital controller (Yuyao, Zhejiang, P.R. China, Model TDA-8002), with an accuracy of $\pm 0.10^{\circ}\text{K}$. The pressure at the exit of the extractor was measured using a pressure gauge with an accuracy of 0.2 MPa. After leaving the extractor, the stream of carbon dioxide loaded with extract flowed through an on/off valve and a sequence of pressure expansion valves (needle valve, Yancheng, Jiangsu, P.R. China, Model WL21H-320P, DW6), in which the stream pressure was reduced down to atmospheric pressure, and the oily extract was recovered in a glass collector. Water and volatile components were deposited in a second collector. The volume of the carbon dioxide was measured by a flowmeter (Changchun Meter Company, Jilin, P.R. China, Model LML-2), with an accuracy of ± 0.01 L.

Figure 3 is the schematic diagram of the SFCF apparatus for extraction of *Hippophae rhamnoides* L. seed oil. It includes an extractor with an internal volume of 1×10^{-3} m³ ($D = 6.6 \times 10^{-2}$ m) and two separators, one with a volume of 1×10^{-3} m³ and the other of 3×10^{-4} m³. CO₂ with a purity of higher than 99.9% was fed by a high-pressure plug pump capable of operating at pressures up to 40 MPa and flow rates up to 8×10^{-3} m³/h of CO₂ (liquid). *Hippophae rhamnoides* L. seeds were milled to a mean particle size of 0.4 to 1.0 mm. The weight of seeds loaded in the extractor was 120 g. The experiments were performed at different

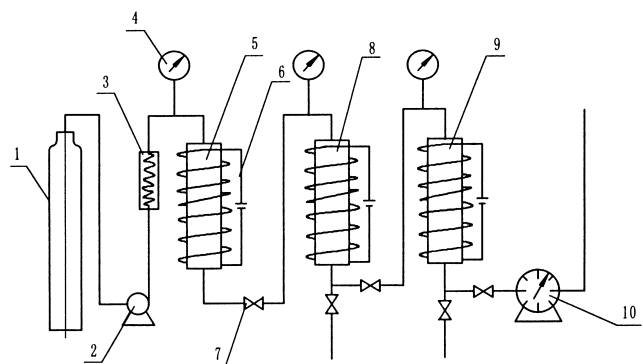


Figure 3. Schematic diagram of experimental apparatus. 1. CO₂ cylinder, 2. pump, 3. preheater, 4. pressure gauge, 5. extractor, 6. electric heating belt, 7. reductor, 8, 9. separator, and 10. rotameter.

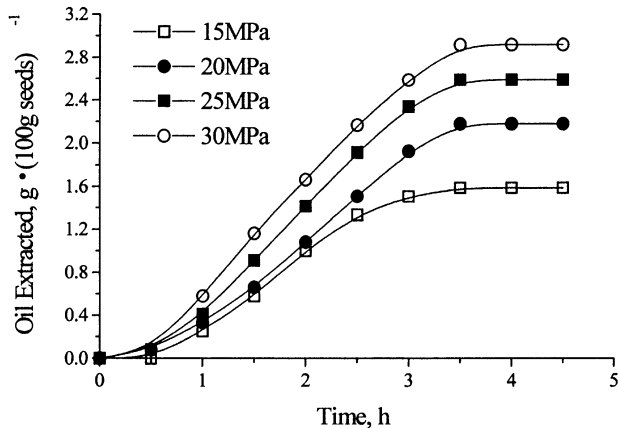


Figure 4. Effects of pressure on extraction, dot = experiment; line = simulation. Experimental conditions: 308°K, 0.1 m³/h, and 18 to 28 mesh (0.643 to 1.033 mm).

flow rates (from 0.05 to 0.2 m³/h, referred to CO₂ gas flow rates in ambient conditions). The oil content of the *Hippophae rhamnoides* L. seed was 5.0 wt%, determined by Soxhlet extraction. The experimental results are shown in Figures 4 through 6.

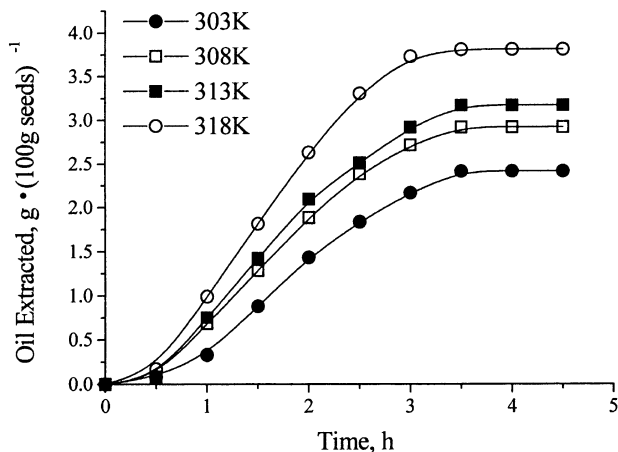


Figure 5. Effects of temperature on extraction, dot = experiment; line = simulation. Experimental conditions: 20 MPa, 0.2 m³/h, and 28 to 36/mesh (0.491 to 0.643 mm).



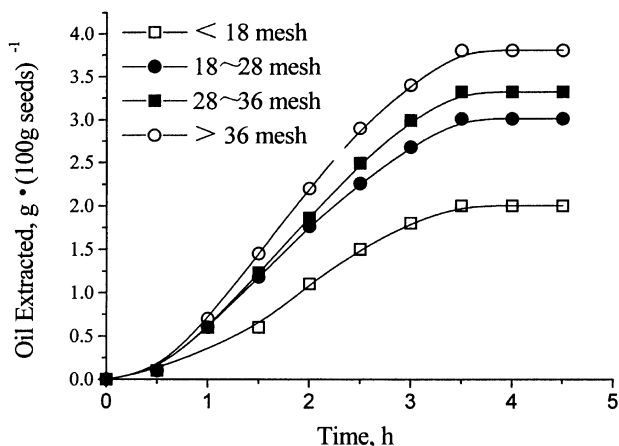


Figure 6. Effects of particle size on extraction, dot = experiment; line = simulation. Experimental conditions: 20 MPa, 313°K, 0.2 m³/h, 18 mesh, 1.033 mm; 28 mesh, 0.643 mm; and 36 mesh, 0.491 mm.

RESULTS AND DISCUSSION

Experimental

To find the optimum operating conditions, the effects of various parameters such as pressure, temperature, extraction time, and particle size, on the oil yield were investigated.

The effect of extraction pressure on the oil yield is shown in Figure 4. The experiments were performed at $T = 308^{\circ}\text{K}$ and various pressures. The particle size was fixed at 18 to 28 mesh and the CO_2 flow rate was $0.1 \text{ m}^3/\text{h}$. From Figure 4, it can be seen that the oil yield increased with pressure. This is because with an increase of pressure, both the density of SCF CO_2 and the solubility of solute increased. Furthermore, according to the P-R equation of state (EOS), change of density with pressure became significant between 5 and 25 MPa. For practical application, we propose that 25 MPa should be employed.

The effect of extraction temperature on the oil yield is illustrated in Figure 5. It can be seen that the oil yield increased with the temperature rise, and attained the maximum value at a temperature of 318°K . When the temperature changed from 303°K to 318°K , the oil yield increased 36.4%.

Figures 4 through 6 show the yield-vs.-time curves under the different operating conditions. It is clear that the extraction process was composed of

two stages: rapid extraction of free solute and slow extraction, mainly controlled by the internal diffusion. The time consumed in the first extraction stage depends both on the solute solubility in SCF CO_2 and on the particle size. Under our experimental conditions, the most amount of seed oil was extracted in the first stage during 150 to 180 min.

Modeling and Simulation

By use of the model to simulate the experimental data, we got satisfactory results when setting $K = 10$ under our operating conditions. The total mean errors between calculation and experimental data were less than 10%. The fitting including the effects of pressure, temperature, and particle size on the extraction rates and the simulation results, are illustrated in Figures 4 through 6. In the SCF extraction of oil from seeds, as much as 75 to 80% of the oil is extracted during the fast period, depending on the degree of milling, hence, on the availability of the liquid oil to the dense gas. The extraction curve is a plot of total mass of oils extracted vs. total extraction time used. From Figures 4 through 6, we also find out that the curves are nearly linear with a slope close to the value of oil solubility in CO_2 (the initial linear part of the extraction curve was not distinct because the rate of extraction diminished from the very start), followed by a transition period, during which, the rate of extraction drops rapidly. The extraction rate became much slower during the final period. When the pressure changed from 15 MPa to 30 MPa, the oil yields were increased as the pressure increased. At 30 MPa, it had the maximum oil yield. Similarly, when the temperature changed from 303°K to 318°K the oil yields were increased as the temperature was increased. At 318°K, it had the maximum oil yield.

CONCLUSION

Hippophae rhamnoides L. seed oil was extracted using supercritical CO_2 with an extraction set-up of 1 L. In this process, many factors impacted on the oil yield, such as pressure, temperature, and extraction time, as well as seed particle size and charge quantity. The optimum conditions were found to be the following: extraction pressure of 20 MPa to 30 MPa, extraction temperature of 35°C to 40°C, supercritical CO_2 flow rate of 0.15 m^3/h to 0.2 m^3/h , and extraction time of 4 to 5 h. Under such a conditions, the oil obtained was very lucid and of good quality.

Modeling the SCF extraction of *Hippophae rhamnoides* L. seed oil was studied based on differential mass balance equations. By a series of transforms and derivatives, the explicit expression of the oil yield, $q(z,t)$,



was presented. It can be used to simulate the SCFE process. In this model, only one adjustable parameter was used: the equilibrium constant between the solvent and the free solute phase K. A satisfactory fitting of the experimental data was obtained by setting K = 10.

Milling of *Hippophae rhamnoides* L. seeds before extraction not only can increase the surface area but also partly releases the solute from the cells. This is of great importance in the extraction oil from seeds where the cell walls are almost impermeable. In this study, for *Hippophae rhamnoides* L. seed oil extraction with SCF CO₂, as much as 75 to 80% of the oil is extracted during the fast period, depending on the degree of milling, hence, on the availability of the liquid oil to the dense gas.

NOMENCLATURE

A	cross section area, m ²
A _p	specific mass transfer area, m ⁻¹
c	solute concentration in fluid phase, kg·kg ⁻¹
c*	solid phase concentration at interfacial boundary, kg·kg ⁻¹
d _p	particle size, mm
D _L	axial dispersion coefficient, m ² ·s ⁻¹
K	equilibrium constant
k _f	solvent phase mass-transfer coefficient
q	solute concentration in solid phase, kg·kg ⁻¹
t	extraction time, s
u	velocity of the supercritical fluid, m·s ⁻¹
z	height of the bed, m

Greek Letters

ε	void fraction
ρ_f	density of solvent, kg·m ⁻³
ρ_s	density of solid phase, kg·m ⁻³

REFERENCES

1. Snyder, J.M.; Friedrich, J.P.; Christianson, D.D. Effect of moisture and particle size on the extractability of oils from seeds with supercritical CO₂. *J. Am. Oil Chem. Soc.* **1984**, *61* (12), 1852–1856.
2. Sovova, H.; Kucera, J.; Jez, J. Rate of the vegetable oil extraction with supercritical CO₂—II. Extraction of grape oil. *Chem. Eng. Sci.* **1994**, *49* (3), 415–420.



3. Fullana, M.; Trabelsi, F.; Recasens, F. Use of neural net computing for statistical and kinetic modeling and simulation of supercritical fluid extractors. *Chem. Eng. Sci.* **1999**, *54* (24), 5845–5862.
4. Sato, M.; Goto, M.; Hirose, T. Fractional extraction with supercritical carbon dioxide for the removal of terpenes from citrus oil. *Ind. Eng. Chem. Res.* **1995**, *34*, 3941.
5. Taniguchi, M.; Tsuji, T.; Shibata, M.; Kobayashi, T. Extraction of oils from wheat germ with supercritical carbon dioxide. *Agric. Biol. Chem.* **1985**, *49* (8), 2367–2372.
6. Sovova, H.; Komers, R. Supercritical carbon dioxide extraction of Caraway essential oil. *Chem. Eng. Sci.* **1994**, *49* (15), 2499–2505.
7. Favati, F.; King, J.W.; Mazzanti, M. Supercritical carbon dioxide extraction of evening primrose oil. *J. Am. Oil Chem. Soc.* **1991**, *68* (6), 422–427.
8. Reverchon, E.; Donsi, G.; Osseo, L.S. Modeling of supercritical fluid extraction from herbaceous matrices. *Ind. Eng. Chem. Res.* **1993**, *32* (11), 2721–2726.
9. Got, M.; Extraction of peppermint oil by supercritical carbon dioxide. *J. Chem. Eng. Jpn.* **1993**, *26* (4), 402–407.
10. Bulley, N.R.; Fattori, M. Supercritical fluid extraction of vegetable oil seeds. *J. Am. Oil Chem. Soc.* **1984**, *61* (8), 1362–1365.
11. Roy, B.C.; Goto, M.; Hirose, T. Extraction of ginger oil with supercritical carbon dioxide: experiments and modeling. *Ind. Eng. Chem. Res.* **1996**, *35* (2), 607.
12. Sovova, H. Rate of the vegetable oil extraction with supercritical CO_2 —I. Modelling of extraction curves. *Chem. Eng. Sci.* **1994**, *49* (3), 409–414.
13. Perrut, M.; Clavier, J.Y.; Poletto, M.; Reverchon, E. Mathematical modeling of sunflower seed extraction by supercritical CO_2 . *Ind. Eng. Chem. Res.* **1997**, *36* (2), 430–435.
14. Reverchon, E.; Daghero, J.; Marrone, C.; Mattea, M.; Poletto, M. Supercritical fractional extraction of fennel seed oil and essential oil: experiments and mathematical modeling. *Ind. Eng. Chem. Res.* **1999**, *38* (8), 3069–3075.
15. Reverchon, E.; Marrone, C. Modeling and simulation of the supercritical CO_2 extraction of vegetable oils. *J. Supercrit. Fluids* **2001**, *19*, 161–175.
16. Cocero, M.J.; Garcia, J. Mathematical model of supercritical extraction applied to oil seed extraction by $\text{CO}_2 +$ saturated alcohol—I. Desorption model. *J. Supercrit. Fluids* **2001**, *20*, 229–243.

Received November 2002

Revised April 2003

